J|A|C|S ARTICLES

Published on Web 08/28/2009

Implementation of High Resolution ^{43}Ca Solid State NMR Spectroscopy: Toward the Elucidation of Calcium Sites in Biological Materials

Danielle Laurencin,*[,†,‡] Christel Gervais,[§] Alan Wong,[†,||] Cristina Coelho,[§] Francesco Mauri,[⊥] Dominique Massiot,[#] Mark E. Smith,[†] and Christian Bonhomme*[,§]

Department of Physics, University of Warwick, Coventry, CV4 7AL, UK, UPMC Univ Paris 06, UMR CNRS 7574, Laboratoire de Chimie de la Matière Condensée de Paris, F-75005 Paris, France, UPMC Univ Paris 06, UMR 7590, Institut de Minéralogie et de Physique des Milieux Condensés, F-75005 Paris, France, and CEMHTI, CNRS UPR 3079, Université d'Orléans, 1D avenue de la Recherche Scientifique, Orléans, France

Received June 4, 2009; E-mail: danielle.laurencin@univ-montp2.fr; christian.bonhomme@upmc.fr

Abstract: Calcium is one of the most abundant cations in living organisms. It is found in the mineral phase of bone and in proteins like calmodulin. However, its exact environment beyond the first coordination sphere is often unknown, thus hampering the understanding of many biological processes. Here, calcium benzoate trihydrate ($Ca(C_6H_5COO)_2 \cdot 3H_2O$) was used as a model for the NMR analysis of calcium sites in biological materials, because of the similarity of its calcium coordination, to water and carboxylate ligands, to that in several calcium-proteins. First, calcium-43 magic angle spinning (MAS) and static NMR spectra of a ^{43}Ca enriched sample were recorded at different magnetic fields, to investigate the electronic environment of calcium. Complex static lineshapes were obtained because of the presence of anisotropic NMR interactions of similar magnitude (chemical shift anisotropy and quadrupolar interaction), and the full interpretation of the spectra required simulations and gauge-including projector augmented wave (GIPAW) DFT calculations. An NMR investigation of the *coordination* environment of Ca^{2+} was carried out, using high resolution ^{13}C−^{43}Ca MAS NMR experiments such as TRAPDOR (transfer of population double resonance) and heteronuclear *J*-spin−echoes. It was shown that despite the weakness of ^{13}C−^{43}Ca interactions, it is possible to discriminate carbon atoms according to their calcium environment. Long-range calcium−carbon correlations were even evidenced by TRAPDOR, reaching distances >5.6 Å. This work demonstrates that by combining solid state NMR experiments, DFT calculations, and simulations, it will be possible to elucidate the electronic and coordination environment of calcium in many important and complex materials.

Introduction

Calcium is an essential element in living organisms. It is the main cation present in the mineral phase of bone[1] and is involved in the control of many important physiological functions such as muscle contraction.[2] Calcium participates in signaling pathways by binding to proteins like parvalbumin[3] or calmodulin,[4] and detailed studies of local changes in Ca^{2+} concentrations have been carried out to try to understand the development of diseases such as Alzheimer's.[5] Calcium is also present in many important natural and man-made materials. Indeed, it is the fifth most abundant element in the Earth's crust,[6] and a great diversity of calcium-containing materials have been manufactured over the years, such as Bioglass, a calcium-silicate glass used in human implants,[7] phenopren calcium, an organic salt developed for pharmaceutical applications,[8] and calcium-phosphate/collagen composites, prepared for bone regeneration.[9]

Since calcium is a key element in biology, and that its presence in many materials has a central impact on their properties, it appears essential to understand in detail its coordination chemistry. However, because it is a metal cation with closed electron shells, few spectroscopic techniques are available to analyze its local environment. In crystalline species, the distance and arrangement of the neighboring atoms can be

[†] University of Warwick.
[‡] Current address: Institut Charles Gerhardt de Montpellier, UMR 5253, CNRS-UM2-ENSCM-UM1, CC 1701, Place Eugène Bataillon, 34095 Montpellier cedex 5, France.
[§] Laboratoire de Chimie de la Matière Condensée de Paris.
[||] Current address: Laboratoire de Structure et Dynamique par Résonance Magnétique, Service de Chimie Moléculaire, DSM/IRAMIS/SCM, Gif-sur-Yvette 91191, France.
[⊥] Institut de Minéralogie et de Physique des Milieux Condensés.
[#] Université d'Orléans.

(1) Weiner, S.; Wagner, H. D. *Annu. Rev. Mater. Sci.* **1998**, *28*, 271.
(2) Davis, J. P.; Tikunova, S. B. *Cardiovasc. Res.* **2008**, *77*, 619.
(3) Means, A. R.; Dedman, J. R. *Nature* **1980**, *285*, 73.
(4) Celio, M. R.; Heizmann, C. W. *Nature* **1981**, *293*, 300.
(5) Kuchibhotla, K. V.; Lattarulo, C. R.; Hyman, B. T.; Bacskai, B. J. *Science* **2009**, *27*, 1211.
(6) Greenwood, N. N.; Earnshaw, A. *Chemistry of the Elements*, 1st ed.; Pergamon Press: Oxford, 1984.
(7) Jones, J. R.; Ehrenfried, L. M.; Hench, L. L. *Biomaterials* **2006**, *27*, 964.
(8) Atassi, F.; Byrn, S. R. *Pharm. Res.* **2006**, *23*, 2405.
(9) Kamakura, S.; Sasaki, K.; Honda, Y.; Masuda, T.; Anada, T.; Kawai, T.; Matsui, A.; Matsui, K.; Echigo, S.; Suzuki, O. *Key Eng. Mater.* **2008**, *361−363*, 1229.

 10.1021/ja904553q CCC: $40.75

determined using X-ray diffraction (XRD). For more disordered materials, ^{43}Ca solid state magic angle spinning (MAS) NMR and Ca K-edge X-ray absorption spectroscopy (XAS) can be used. In the vast majority of compounds, calcium is directly surrounded by oxygen atoms, and the average position of these atoms can be deduced from the ^{43}Ca isotropic chemical shift δ_{iso}[10−16] or by fitting the Extended X-ray Absorption Fine Structure (EXAFS) spectra.[17−19] Additional information on the distortion of the CaO_x polyhedron ($x = 5-8$) can be accessed by looking at the intensity of the pre-edge in the X-ray Absorption Near Edge Structure (XANES) spectra.[20] However, elucidating calcium environments *beyond* the first coordination sphere is still a real challenge for noncrystalline samples. For instance, only last year was it demonstrated that the ^{43}Ca δ_{iso} provides qualitative information about the nature of the second nearest neighbors for inorganic materials containing Ca−O bonds.[10] Furthermore, Ca K-edge EXAFS spectra seldom provide such information, because of the absence of long-range ordering and the presence of several different backscatterers in the more distant shells, hampering unambiguous fitting of the data.

^{43}Ca NMR is experimentally very challenging. ^{43}Ca is a spin-$^7/_2$ quadrupolar nucleus with a very low natural abundance (∼0.14%) and small gyromagnetic ratio γ_{Ca},[10−16,21,22] making it $\sim 10^5$ times less sensitive than ^1H. Nevertheless, several solution NMR studies of calcium proteins have been carried out, showing that solution ^{43}Ca NMR experiments provide information about the affinity of calcium for the binding site (through the value of the calcium-binding constant) and on the chemical nature and geometry of the Ca^{2+} coordination sphere (through the ^{43}Ca isotropic chemical shift and quadrupole coupling constant, which vary for different classes of Ca^{2+} binding motifs).[23−25] However, such experiments do not allow the exact arrangement of the different ligands around the metal nor the possible influence of more distant organic fragments on the accessibility of calcium sites in proteins to be analyzed. Thus, because of the importance of calcium in biological systems, much effort is being made to further develop ^{43}Ca solid state NMR. Indeed, solid state NMR is a site-specific probe, and *all* relevant NMR interactions—quadrupolar interaction, chemical shift anisotropy (CSA), as well as dipolar couplings and *J* couplings—can in principle be used as potential spies to extract valuable structural information. This is especially true in the case of ^{43}Ca, because of its small quadrupole moment. Indeed, in contrast with other quadrupolar nuclei such as ^{25}Mg, for which the quadrupolar interaction usually completely dominates the spectra,[21] the few static ^{43}Ca NMR experiments carried out so far on the three polymorphs of calcium carbonate,[12,16] have shown that a small contribution of the CSA needs to be taken into account to fully simulate the ^{43}Ca static lineshapes, and that it is possible to determine not only the CSA parameters, but also the relative orientation of ^{43}Ca quadrupolar and CSA tensors.

To the best of our knowledge, no static NMR experiments have yet been carried out to determine the local *electronic environment* of Ca^{2+} in metalloproteins or biomaterials, despite the fact that recent computational studies have shown that it would clearly be worth determining both ^{43}Ca quadrupolar *and* CSA parameters in these compounds, because they can provide information on the geometrical arrangement of the nuclei directly bound to the metal ion.[11,12] This is not wholly surprising given the experimental difficulties which arise when it comes to studying low-γ quadrupolar nuclei[21] such as ^{43}Ca, ^{25}Mg or ^{67}Zn, especially when their concentration in the samples is low. For instance, Ellis and Lipton have designed cryogenic probes to increase the signal strength to specifically look at dilute Mg^{2+} and Zn^{2+} sites in metalloproteins.[26] They showed that the ^{67}Zn and ^{25}Mg quadrupolar parameters extracted from static NMR spectra can bring insight into the environment of Zn^{2+} and Mg^{2+} cations in proteins like human carbonic anhydrase[27] or the DNA Repair Protein Apurinic/Apyrimidic Endonuclease[28] and shed light on their biological role. Similarly, it would thus be worth trying to characterize the local electronic environment of calcium in proteins and biomaterials using CSA and quadrupolar parameters.

To fully describe the local structure around calcium sites, it is also necessary to determine the exact *coordination environment* of the cation beyond the first coordination sphere, by analyzing which nuclei are in its vicinity and trying to discriminate them according to their distance or binding mode. As previously mentioned, solid state NMR can be used to answer these questions: over the past 20 years, several robust high-resolution NMR sequences have been developed which allow through-space proximities (involving dipolar couplings) and through-bond connectivities (involving *J* couplings) *between* spin $^1/_2$ and quadrupolar nuclei to be analyzed.[21,29] However, probing distances between calcium and neighboring spins X is very challenging because of the weakness of the dipolar couplings involved (proportional to $(\gamma_X\gamma_{Ca})/r^3$, where r represents the through-space distance between the two nuclei). It is only very recently that it has been shown that high-resolution solid state NMR experiments can help investigate calcium-proton proximities in synthetic ^{43}Ca-labeled hydroxyapatite and oxy-hydroxyapatite phases, by reintroducing $^{43}Ca\cdots{}^1H$ dipolar

(10) Gervais, C.; Laurencin, D.; Wong, A.; Pourpoint, F.; Woodward, B.; Howes, A. P.; Pike, K. J.; Dupree, R.; Mauri, F.; Bonhomme, C.; Smith, M. E. *Chem. Phys. Lett.* **2008**, *464*, 42.
(11) Wong, A.; Laurencin, D.; Wu, G.; Dupree, R.; Smith, M. E. *J. Phys. Chem. A* **2008**, *112*, 9807.
(12) Bryce, D. L.; Bultz, E. B.; Aebi, D. *J. Am. Chem. Soc.* **2008**, *130*, 9282.
(13) Angeli, F.; Gaillard, M.; Jollivet, P.; Charpentier, T. *Chem. Phys. Lett.* **2007**, *440*, 324.
(14) Wong, A.; Howes, A. P.; Dupree, R.; Smith, M. E. *Chem. Phys. Lett.* **2006**, *427*, 201–205.
(15) Lin, Z.; Smith, M. E.; Sowrey, F. E.; Newport, R. J. *Phys. Rev. B.* **2004**, *69*, 224107.
(16) Dupree, R.; Howes, A. P.; Kohn, S. C. *Chem. Phys. Lett.* **1997**, *276*, 399.
(17) Skipper, L. J.; Sowrey, F. E.; Pickup, D. M.; Fitzgerald, V.; Rashid, R.; Drake, K. O.; Lin, Z.; Saravanapavan, P.; Hench, L. L.; Smith, M. E.; Newport, R. J. *J. Biomed. Mat. Res., Part A* **2004**, *70A*, 354.
(18) Peters, F.; Schwarz, K.; Epple, M. *Thermochim. Acta* **2000**, *361*, 131.
(19) Harries, J. E.; Hukins, D. W. L.; Hasnain, S. S. *Calcif. Tissue Int.* **1988**, *43*, 250.
(20) Cormier, L.; Neuville, D. R. *Chem. Geol.* **2004**, *213*, 103.
(21) MacKenzie, K. J. D.; Smith, M. E. *Multinuclear Solid State NMR of Inorganic Materials*; Pergamon: Oxford, 2002.
(22) Smith, M. E. *Annu. Rep. NMR Spectrosc.* **2001**, *43*, 121.
(23) Aramini, J. M.; Vogel, H. J. *Biochem. Cell. Biol.* **1998**, *76*, 210 (and references therein).
(24) Drakenberg, T.; Johansson, C.; Forsén, S. *Methods Mol. Biol.* **1997**, *60*, 299.
(25) Forsén, S.; Johansson, C.; Linse, S. *Methods Enzymol.* **1993**, *227*, 107.
(26) Lipton, A. S.; Heck, R. W.; Sears, J. A.; Ellis, P. D. *J. Magn. Reson.* **2004**, *168*, 66.
(27) Lipton, A. S.; Heck, R. W.; Sears, J. A.; Ellis, P. D. *J. Am. Chem. Soc.* **2004**, *126*, 4735.
(28) Lipton, A. S.; Heck, R. W.; Primak, S.; McNeill, D. R.; Wilson, D. M., III; Ellis, P. D. *J. Am. Chem. Soc.* **2008**, *130*, 9332.
(29) Amoureux, J. P.; Trebosc, J.; Delevoye, L.; Lafon, O.; Hu, B.; Wang, Q. *Sol. St. Nucl. Magn. Reson.* **2009**, *35*, 12.

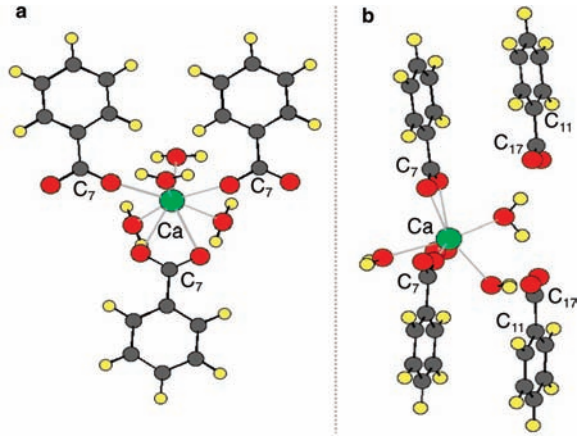

Figure 1. Representations of the calcium environment in $Ca(C_6H_5COO)_2 \cdot 3H_2O$. Ca, C, O and H atoms are represented in green, gray, red and yellow respectively. (a) View of the benzoate ligands and water molecules directly bound to calcium. (b) View of the positioning of the more distant benzoate anions in the crystal structure.

couplings ~425 Hz:[30−32] $^{43}Ca-^{1}H$ Rotational-Echo DOuble Resonance (REDOR) experiments allowed the Ca(2) site of hydroxyapatite (which is the only one bound to an OH group) to be distinguished from the Ca(1) site. High resolution ^{43}Ca NMR spectroscopy would be worth developing to try to analyze the arrangement of other second-nearest neighbors X around calcium, and notably carbon, which is one of the main elements in biomolecules. However, probing $^{43}Ca-^{13}C$ dipolar couplings appears challenging because of the weakness of the interactions involved (~85 Hz for a Ca···C distance ~2.9 Å, typically found for a carboxylate directly bound to Ca^{2+} in a bidentate mode), and looking at through-bond $^{43}Ca-O-^{13}C$ connectivities appears as even more difficult, due to the ionic-character of Ca−O bonds.

The purpose of this article is to evaluate the potential of ^{43}Ca solid state NMR, for the structural analysis of calcium in biolike environments. Two key issues are addressed: (i) how can static ^{43}Ca NMR spectra be interpreted and used to help understand the local electronic environment of Ca^{2+}, and (ii) is it possible to analyze $^{43}Ca\cdots{}^{13}C$ through-space and through-bond interactions, in order to help describe the coordination environment of the cation? To answer these questions, the complete ^{43}Ca NMR study of a model compound was carried out, calcium benzoate trihydrate ($*Ca(C_6H_5COO)_2 \cdot 3H_2O$, 60% ^{43}Ca-labeled) (see Figure 1 and supplementary Figure S1, from hereon, "S" will refer to the Supporting Information). This compound was chosen because it contains Ca^{2+} coordinated to carboxylate groups and water molecules, that is, to ligands similar to those found in the environment of calcium in proteins such as calmodulin,[3] parvalbumin,[4] or human α-Lactalbumin.[33]

In the first part of the paper, results of ^{43}Ca static and MAS NMR studies of ^{43}Ca-labeled $*Ca(C_6H_5COO)_2 \cdot 3H_2O$ are presented. Experiments were carried out at different magnetic fields, and the importance of computer simulations and of GIPAW[34] DFT calculations is underscored, by demonstrating how they can help interpret the complex static lineshapes and elucidate the electronic structure around Ca^{2+} in protein-like environments. In the second part, we report on high-resolution $^{43}Ca-^{13}C$ double resonance experiments. Differences in calcium−carbon interactions were evidenced using robust NMR sequences like $^{13}C\{^{43}Ca\}$ TRAPDOR (TRAnsfer of Population DOuble Resonance) and heteronuclear *J*-spin−echoes, and it is shown how these sequences can be used to describe the environment of Ca^{2+} beyond the first coordination sphere, and to access information on relative $^{13}C-^{43}Ca$ internuclear distances.

Experimental and Computational Details

1. Synthesis, IR and XRD Characterization. Sixty percent ^{43}Ca enriched $*CaCO_3$ (CortecNet) was used as a source of labeled calcium. Two syntheses were performed, with either 100% ^{13}C-enriched C_6H_5*COOH (labeled only on the carboxylic acid function, provided by Aldrich) or nonlabeled C_6H_5COOH (Aldrich). Distilled water and reagent grade solvents were used throughout the reactions. Both $*Ca(C_6H_5*COO)_2 \cdot 3H_2O$ and $*Ca(C_6H_5COO)_2 \cdot 3H_2O$ were prepared using the same procedure, thus only the quantities used for the synthesis of the former compound are reported here.

$*CaCO_3$ (100 mg, 0.98 mmol) was heat treated at 1000 °C for 3 h under Ar to form *CaO, and the resulting powder was suspended in 2 mL of distilled water. A solution of C_6H_5*COOH was prepared by dissolving 242 mg of C_6H_5*COOH (1.96 mmol, 2 equiv) in a mixture of 2 mL of H_2O and 4 mL of CH_3OH, and was added dropwise to the "*CaO" suspension, which progressively became clearer. The mixture was heated to 90 °C, to completely dissolve any remaining solid residues, and to reduce the volume by half. Slow cooling down to room temperature subsequently led to the formation of needle-shaped crystallites of $*Ca(C_6H_5*COO)_2 \cdot 3H_2O$, which were separated and dried with diethylether (270 mg, ~80% yield).

The compounds were characterized by IR and X-ray powder diffraction (see Figure S2). IR spectra were recorded from KBr pellets on a Perkin-Elmer GX FTIR spectrometer between 400 and 4000 cm^{-1}. X-ray diffraction patterns were collected at room temperature with a PANAnalytical X'Pert Pro MPD X(G23) diffractometer using Cu Kα radiation. Measurements were performed in the 2θ range between 5 and 60°, with a step size of 0.013°.

2. Solid State NMR Experiments. ^{43}Ca solid state NMR experiments were performed at 9.4 T ($\nu_0(^{43}Ca) = 26.93$ MHz) on a Bruker Avance II 400 NMR spectrometer, 11.75 T ($\nu_0(^{43}Ca) = 33.66$ MHz) on a Bruker Avance III 500 NMR spectrometer, and 14.1 T ($\nu_0(^{43}Ca) = 40.38$ MHz) on a Bruker Avance II^+ 600 NMR spectrometer. The ^{43}Ca magic angle spinning (MAS) NMR spectrum of $*Ca(C_6H_5*COO)_2 \cdot 3H_2O$ was recorded at 11.75 T, with a Bruker 4 mm triple resonance MAS probe spinning at 12.5 kHz. 3600 transients were acquired using a recycle delay of 4 s, and 100 kHz spinal-64 ^{1}H decoupling was applied during acquisition. The magic angle was precisely set by analyzing the line shape of the satellite transitions of 60% ^{43}Ca labeled calcite $*CaCO_3$, and simulating it with SIMPSON[35] (Figure S3). ^{43}Ca chemical shifts were all referenced to a 1 $mol \cdot L^{-1}$ solution of $CaCl_2$.[10,36]

In the case of the unenriched COO^- derivative $*Ca(C_6H_5COO)_2 \cdot 3H_2O$, ^{43}Ca static NMR spectra were recorded at 11.75 and 14.1 T using Bruker 4 mm triple resonance probes. A recycle delay of 4 s was used, and 70 kHz continuous wave (CW) ^{1}H decoupling was applied during the acquisition. 9800 and 11000 transients were acquired at 14.1 and 11.75 T, respectively. The ^{43}Ca static NMR

(30) Laurencin, D.; Wong, A.; Dupree, R.; Hanna, J. V.; Smith, M. E. *J. Am. Chem. Soc.* **2008**, *130*, 2412.
(31) Laurencin, D.; Wong, A.; Dupree, R.; Smith, M. E. *Magn. Reson. Chem.* **2008**, *46*, 347.
(32) Wong, A.; Laurencin, D.; Dupree, R.; Smith, M. E. *Solid State Nucl. Magn. Reson.* **2009**, *35*, 32.
(33) Acharya, K. R.; Ren, J.; Stuart, D. I.; Phillips, D. C.; Fenna, R. E. *J. Mol. Biol.* **1991**, *221*, 571.
(34) Pickard, C. J.; Mauri, F. *Phys. Rev. B,* **2001**, *63*, 245101.
(35) Bak, M.; Rasmussen, J. T.; Nielsen, N. C. *J. Magn. Reson.* **2000**, *147*, 296.
(36) Trokiner, A.; Bessière, A.; Thouvenot, R.; Hau, D.; Marko, J.; Nardello, V.; Pierlot, C.; Aubry, J. M. *Solid State Nucl. Magn. Reson.* **2004**, *25*, 209.

spectra of the doubly labeled compound *Ca(C_6H_5*COO)$_2\cdot 3H_2O$ were also recorded at 9.4 and 11.75 T using Bruker 4 mm triple resonance probes. A recycle delay of 4 s was used and CW ^1H decoupling was applied during the acquisition. 10800 transients were acquired at both magnetic fields. At 9.4 T, a second experiment involving CW decoupling of both ^1H *and* ^{13}C was performed, in which 12 600 transients were acquired. Table S1 summarizes all the experimental conditions used to record the ^{43}Ca static and MAS NMR spectra.

The ^{13}C MAS and $^{13}C\{^1H\}$ cross-polarization (CP) MAS NMR spectra of *Ca($C_6H_5COO)_2\cdot 3H_2O$ and *Ca(C_6H_5*COO)$_2\cdot 3H_2O$ were recorded on a Bruker Avance III 500 spectrometer (11.75 T, $\nu_0(^1H) = 500.78$ MHz, $\nu_0(^{13}C) = 125.78$ MHz), using a Bruker 4 mm MAS probe, and spinning at 10 kHz. For the CPMAS experiments, ramped-amplitude CP[37] was used on the ^1H channel to transfer efficiently magnetization from ^1H to ^{13}C, and the contact time was set to 8 ms. 100 kHz spinal-64 ^1H decoupling was applied during the acquisition.[38] ^{13}C chemical shifts were referenced to tetramethylsilane (TMS).

The $^1H/^{13}C/^{43}Ca$ MAS experiments were recorded on a Bruker Avance II 400 spectrometer (9.40 T, $\nu_0(^{13}C) = 100.61$ MHz, $\nu_0(^{43}Ca) = 26.93$ MHz). A Bruker 4 mm triple resonance MAS probe was used, spinning at 10 kHz. Schemes representing the different correlation experiments, as well as details concerning the delays and phase cycling used, are given in Figure S4. For the enriched *COO^- derivative, no $^1H/^{13}C$ CP transfer was applied during the TRAPDOR[21,39] and heteronuclear *J* spin−echo experiments. However, a saturation loop was implemented systematically before the recycle delay, and in the case of the heteronuclear *J*-spin−echoes, a further 16 dummy scans were added. In the case of the unenriched COO^- derivative *Ca($C_6H_5COO)_2\cdot 3H_2O$, a ramp CP step was added to the TRAPDOR sequence.

It is worth noting that for both the TRAPDOR and heteronuclear *J*-spin−echo experiments, the optimisation of the spinal-64 ^1H decoupling is crucial, as it actually dictates the possibility to reach "long" ^{13}C dephasing times, and thus the ability to evidence very weak $^{13}C-^{43}Ca$ interactions. The efficiency of the spinal-64 decoupling scheme was systematically optimized by recording series of ^{13}C echo spectra. Finally, it should be noted that the fact that the TRAPDOR experiments were carried out on the non-^{13}C-labeled compound is of paramount importance for the interpretation of the data, because it ensures the absence of any residual $^{13}C-^{13}C$ homonuclear dipolar couplings, which would have been a severe drawback for the safe estimation of the $^{43}Ca-^{13}C$ interactions and evaluation of the internuclear distances.

3. GIPAW Calculations. The first principles calculations based on the GIPAW method[34] were performed within Kohn−Sham DFT using the PARATEC code.[40] The crystalline structure is described as an infinite periodic system using periodic boundary conditions. The NMR calculations are performed as follows: partial geometry optimizations were carried out, starting from the experimental structure[41] and allowing the positions of the hydrogen atoms to relax using DFT calculation.[42,43] The new coordinates obtained after relaxation are summarized in Table S2. The PBE generalized gradient approximation[44] was used and the valence electrons were described by norm conserving pseudopotentials[45] in the Kleinman−Bylander[46] form.

The core definition for O and C is $1s^2$, and it is $1s^22s^22p^6$ for Ca. The core radii are 1.2 au for H, 1.45 au for Ca, 1.5 au for O and 1.6 au for C. The wave functions are expanded on a plane wave basis set with a kinetic energy cutoff of 80 Ry. The isotropic chemical shift δ_{iso} is defined as $\delta_{iso} = -[\sigma - \sigma^{ref}]$ where σ is the isotropic shielding and σ^{ref} is the isotropic shielding of the same nucleus in a reference system as previously described.[10,42] Diagonalization of the symmetrical part of the calculated shielding tensor provides its principal components δ_{11}, δ_{22} and δ_{33} defined so that $|\delta_{33} - \delta_{iso}| \geq |\delta_{11} - \delta_{iso}| \geq |\delta_{22} - \delta_{iso}|$, and $\delta_{iso} = 1/3(\delta_{11} + \delta_{22} + \delta_{33})$. The CSA parameters are defined by $\Delta_{CS} = \delta_{33} - \delta_{iso}$ and $\eta_{CS} = |(\delta_{22} - \delta_{11})/\Delta_{CS}|$. The principal components V_{xx}, V_{yy} and V_{zz} of the electric field gradient (EFG) tensor defined with $|V_{zz}| \geq |V_{xx}| \geq |V_{yy}|$ are obtained by diagonalization of the tensor. The quadrupolar interaction can then be characterized by the quadrupolar coupling constant C_Q and the asymmetry parameter η_Q, which are defined as $C_Q = eQV_{zz}/h$ and $\eta_Q = (V_{yy} - V_{xx})/V_{zz}$. The program outputs both tensors in the crystal axis system. Absolute orientation in the molecular frame of the shielding and EFG tensors, as well as their relative orientation, can therefore be obtained.

4. Simulations. Simulations of the NMR spectra were carried out using different freely available softwares which take into account the quadrupolar interaction, anisotropic chemical shifts and dipolar interaction: SIMPSON[35] and dmfit,[47] through its QUASAR[48] or Int2Q_D models. The tensors describing the different anisotropic interactions were all oriented in the EFG principal axis frame (PAS). The quadrupolar interaction is defined by C_Q (or $|V_{zz}|$) and η_Q. The chemical shift tensor is characterized by δ_{iso}, Δ_{CS}, η_{CS} and three angles $\{\varphi,\chi,\psi\}$. Each dipolar coupling is characterized by its intensity in Hz (D) and the $\{\alpha_D, \beta_D\}$ set of Euler angles. Thus, eight independent parameters need to be used to characterize a single site when only the quadrupolar and CSA interactions are taken into account in the simulations, while 17 are necessary when 3 additional heteronuclear dipolar couplings are considered. Additional information on the different softwares (including the Euler angle conventions) and on the way simulations were carried out are given in the Supporting Information (section C1).

Results and Discussion

1. Analysis of the Electronic Environment of Calcium, using ^{43}Ca NMR Experiments, Simulations and GIPAW Calculations. The crystal structure of Ca($C_6H_5COO)_2\cdot 3H_2O$ consists of a single calcium site, in which the cation is coordinated to eight oxygen atoms belonging to four water molecules and three carboxylate groups (Figure 1).[41] The benzoate ligands bound to calcium are crystallographically equivalent, and their phenyl rings are located in the same plane as Ca^{2+}. As shown in Figures 1b and S1, there is a second group of benzoate anions in the crystal structure, which are not coordinated to Ca^{2+}, and which form a layer parallel to the previous one.

^{43}Ca MAS and static NMR experiments were first carried out on this compound in order to access the ^{43}Ca quadrupolar and CSA parameters, providing information about the electronic environment around calcium. Experiments were performed on

(37) Metz, G.; Wu, X. L.; Smith, S. O. *J. Magn. Reson.* **1994**, *A 110*, 219.
(38) Fung, B. M.; Khitrin, A. K.; Ermolaev, K. *J. Magn. Reson.* **2000**, *142*, 97.
(39) Grey, C. P.; Vega, A. J. *J. Am. Chem. Soc.* **1995**, *117*, 8232.
(40) Pfrommer, B., Raczkowski, D., Canning, A., Louie, S. G. *PARATEC (PARAllel Total Energy Code)*; Lawrence Berkeley National Laboratory (with contributions from Mauri, F., Cote, M., Yoon, Y., Pickard, C., Heynes, P.). For more information see www.nersc.gov/projects/paratec.
(41) Senkovska, I.; Thewalt, U. *Acta Cryst. C* **2005**, *61*, m448.
(42) Gervais, C.; Profeta, M.; Lafond, V.; Bonhomme, C.; Azaïs, T.; Mutin, P. H.; Pickard, C. J.; F.; Mauri, F.; Babonneau, F. *Magn. Reson. Chem.* **2004**, *42*, 445.
(43) Gervais, C.; Dupree, R.; Pike, K. J.; Bonhomme, C.; Profeta, M.; Pickard, C. J.; Mauri, F. *J. Phys. Chem. A* **2005**, *109*, 6960.
(44) Perdew, J. P.; Burke, K.; Ernzerhof, M. *Phys. Rev. Lett.* **1996**, *77*, 3865.
(45) Troullier, N.; Martins, J. L. *Phys. Rev. B* **1991**, *43*, 1993.
(46) Kleinman, L.; Bylander, D. *Phys. Rev. Lett.* **1982**, *48*, 1425.
(47) Massiot, D.; Fayon, F.; Capron, M.; King, I.; Le Calvé, S.; Alonso, B.; Durand, J.-O.; Bujoli, B.; Gan, Z.; Hoatson, G. *Magn. Reson. Chem.* **2002**, *20*, 70. See also: http://www.cemhti.cnrs-orleans.fr/.
(48) QUASAR module by Jean-Paul Amoureux (UCSS Lille, France) http://www.cemhti.cnrs-orleans.fr/Dmfit/help/Models/QUASAR.aspx.

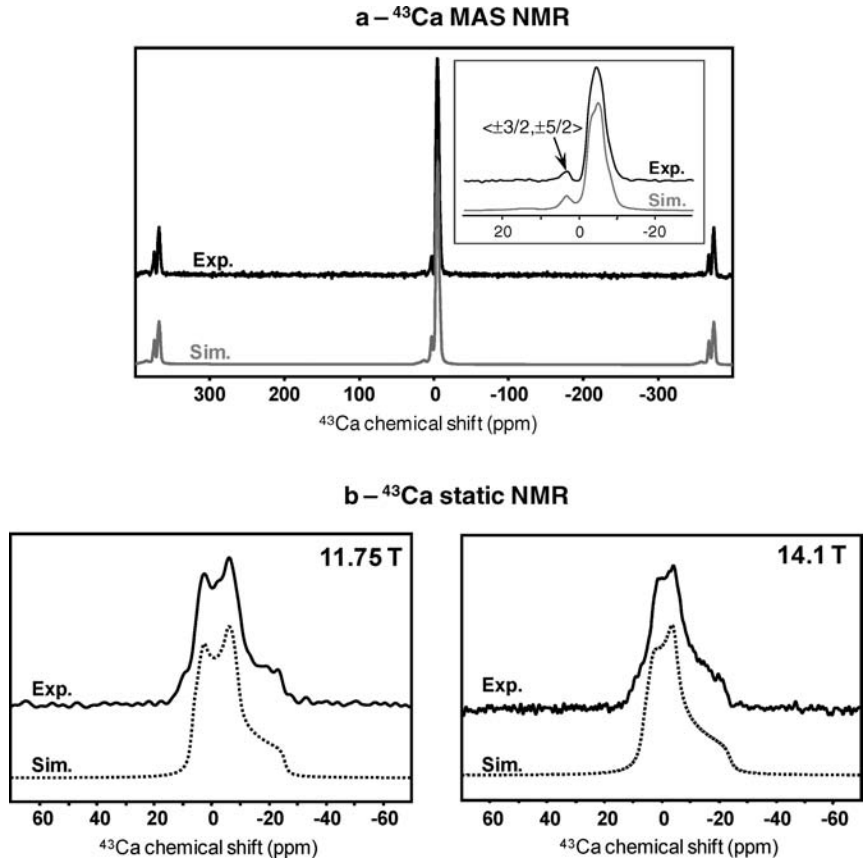

Figure 2. ^{43}Ca NMR spectra of calcium benzoate trihydrate. (a) ^{43}Ca MAS NMR spectrum of *Ca(C_6H_5*COO)$_2$·3H_2O recorded at 11.75 T (top), and its simulation using QUASAR (bottom). Only the first set of spinning sidebands due to the satellite transitions is shown. The inset represents a zoom on the central part of the spectrum, where the central transition and the isotropic component of the $\langle \pm 3/2, \pm 5/2 \rangle$ transition appear. (b) Static ^{43}Ca NMR spectra of *Ca($C_6H_5COO)_2$·3H_2O recorded at 11.75 and 14.1 T, using high power CW {^{1}H} decoupling, and their simulation using QUASAR. For both simulations, the following parameters were used: $\delta_{iso} = -2.5$ ppm, $\Delta_{CS} = -14.0$ ppm, $\eta_{CS} = 0.2$, $\{\varphi,\chi,\psi\} = \{-10°, -62°, 50°\}$, $C_Q = 1.10$ MHz, $\eta_Q = 0.7$.

60% ^{43}Ca-labeled Ca($C_6H_5COO)_2$·3H_2O samples, because the very low natural abundance of ^{43}Ca would have made the measurements unreasonably time-consuming at "low" magnetic fields (9.4 and 11.75 T).[10] Two different calcium benzoate trihydrate phases were synthesized, with and without additional ^{13}C-labeling on the carboxylate carbons C_7 and C_{17} (see experimental details). They were both obtained as crystalline materials, as indicated by their XRD powder patterns (Figure S2), and from hereon will be referred to as *Ca(C_6H_5*COO)$_2$·3H_2O and *Ca($C_6H_5COO)_2$·3H_2O, respectively.

The ^{43}Ca MAS NMR spectrum of *Ca(C_6H_5*COO)$_2$·3H_2O is shown in Figure 2a. A single narrow nearly featureless signal is observed, as it is often the case for ^{43}Ca MAS NMR.[10,11,14−16] However, sidebands corresponding to the various satellite transitions are clearly present, as well as a small isotropic band corresponding to the $< \pm 3/2, \pm 5/2>$ transition. The latter peak, which is very sensitive to the precise setting of the magic angle, allowed the ^{43}Ca MAS spectrum to be simulated very accurately, and the NMR parameters which were derived for the unique ^{43}Ca crystallographic site are $\delta_{iso} = -2.5 \pm 0.2$ ppm, $C_Q = 1.10 \pm 0.05$ MHz and $\eta_Q = 0.7 \pm 0.1$.

To derive precise CSA parameters and gain information on the relative orientation of the ^{43}Ca quadrupolar and CSA tensors, static NMR spectra of *Ca($C_6H_5COO)_2$·3H_2O were recorded at different magnetic fields. As shown in Figure 2b, the experimental lineshapes suggest the presence of both quadrupolar and CSA interactions of similar magnitude.[49−51] This is further illustrated in Figure 3a. Indeed, starting from δ_{iso} and the quadrupolar parameters extracted from the MAS experiments, the simulated static spectrum at 11.75 T is very different from the experimental one. Extensive simulations of the static NMR spectra of calcium benzoate were thus carried out, including both quadrupolar and CSA effects. The best fits obtained at 11.75 and 14.1 T are shown in Figure 2b. The CSA parameters were estimated as $\Delta_{CS} = -14.0 \pm 1.0$ ppm and $\eta_{CS} = 0.2 \pm 0.1$, and the Euler angles orienting the CSA tensor in the quadrupolar PAS as $\varphi = -10° \pm 5°$, $\chi = -62° \pm 5°$, and $\psi = 55° \pm 10°$. Additional simulations confirm the quality of the fit and the precise determination of these angles, because changes in $\{\varphi,\chi,\psi\}$ strongly affect the simulated ^{43}Ca line shape (Figure 3b−d).

As shown here, even in the case of a simple model compound like Ca($C_6H_5COO)_2$·3H_2O, static ^{43}Ca NMR lineshapes can be complex because of the presence of CSA and quadrupolar interactions which are weak and of very similar magnitude. Thus, the interpretation of spectra obtained for calcium sites in "real" biological samples is expected to be challenging, all the more if additional disorder around the metal causes a small chemical shift distribution and smoothes out the spectral

(49) Bryce, D. L.; Bultz, E. B. *Chem.—Eur. J.* **2007**, *13*, 4786.
(50) Kwan, I. C. M.; Mo, X.; Wu, G. *J. Am. Chem. Soc.* **2007**, *129*, 2398.
(51) Yamada, K.; Honda, H.; Yamazaki, T.; Yoshida, M. *Solid State NMR* **2006**, *30*, 162.

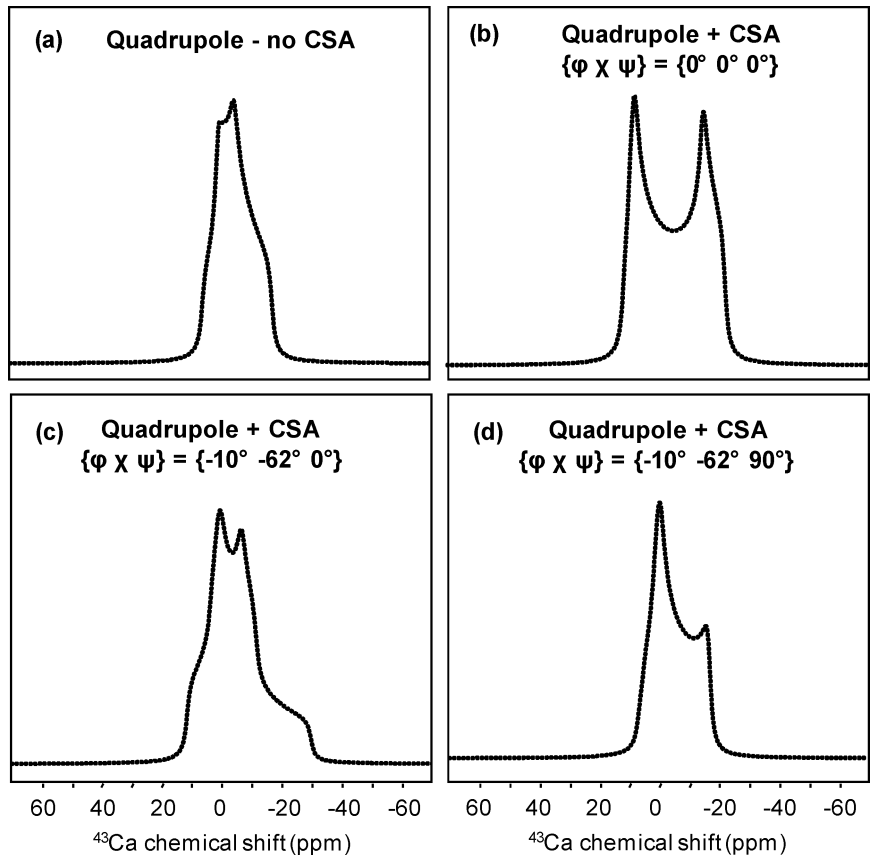

Figure 3. Simulations of the ^{43}Ca static NMR spectrum of $Ca(C_6H_5COO)_2 \cdot 3H_2O$ at 11.75 T. The simulations were carried out using QUASAR, with: (a) $\Delta_{CS} = 0$ ppm; (b) $\Delta_{CS} = -14.0$ ppm and $\{\varphi,\chi,\psi\} = \{0°,0°,0°\}$; (c) $\Delta_{CS} = -14.0$ ppm and $\{\varphi,\chi,\psi\} = \{-10°,-62°,0°\}$; (d) $\Delta_{CS} = -14.0$ ppm and $\{\varphi,\chi,\psi\} = \{-10°,-62°,90°\}$. The experimental spectrum is shown in Figure 2b.

features. To help elucidate the local environment around such calcium sites, one of the possibilities would consist in modeling the structure of the material computationally, calculating the NMR parameters of calcium in the model, and comparing them to the experimental data.[52−54] For such an approach to be robust, it is thus crucial to be able to calculate the NMR parameters accurately. The first extensive calculations of ^{43}Ca NMR parameters were reported in 2008.[10−12] On the one hand, Wong showed that NMR calculations of Ca-*organic* species, including calcium sites in proteins, can be carried out using the so-called "cluster" DFT approach, in which only the closest atoms around the calcium site are considered.[11] Gervais and Bryce both showed alternatively that periodic calculations using the GIPAW method are well adapted to the computation of ^{43}Ca NMR parameters in *inorganic* Ca-compounds.[10,12] In both cases, it was demonstrated that $\delta_{iso}(^{43}Ca)$ and quadrupolar parameters can be reproduced with a fairly good accuracy, and that these NMR parameters can shed light on the electronic environment and local structure around calcium.

Given the high reliability of the GIPAW method and its increasing popularity for the calculation of all NMR parameters of a wide range of nuclei (isotropic chemical shifts, CSA, quadrupolar parameters, and more recently *J*-couplings),[59−63] it is tested here in the case of Ca-*organic* compounds like calcium benzoate. The calculated δ_{iso} and C_Q of $Ca(C_6H_5COO)_2 \cdot 3H_2O$ ($\delta_{iso} = 6.3$ ppm and $C_Q = 0.87$ MHz) were found to differ slightly from the experimental values (−2.5 ppm and 1.10 MHz). Such differences are nevertheless acceptable: indeed, considering the overall ^{43}Ca chemical shift scale,[10,21] δ_{iso} is actually only overestimated by ∼4%; furthermore, these δ_{iso} and C_Q values remain largely in the range expected for calcium carboxylate complexes.[11,14] On the other hand, the CSA parameters and Euler angles calculated using GIPAW ($\Delta_{CS} = -15.4$ ppm, $\eta_{CS} = 0.35$ and $\{\varphi,\chi,\psi\} = \{4°,-62°,65°\}$) were found to be in very good agreement with those extracted from the simulations. This suggests that GIPAW calculations should

(52) Vasconcelos, F.; Cristol, S.; Paul, J.-F.; Tricot, G.; Amoureux, J.-P.; Montagne, L.; Mauri, F.; Delevoye, L. *Inorg. Chem.* **2008**, *47*, 7327.
(53) Charpentier, T.; Ispas, S.; Profeta, M.; Mauri, F.; Pickard, C. J. *J. Phys. Chem. B* **2004**, *108*, 4147.
(54) Tielens, F.; Gervais, C.; Lambert, J. F.; Mauri, F.; Costa, D. *Chem. Mater.* **2008**, *20*, 3336.
(55) Ashbrook, S. E.; Cutajar, M.; Pickard, C. J.; Walton, R. I.; Wimperis, S. *Phys. Chem. Chem. Phys.* **2008**, *10*, 5754.
(56) Uldry, A.-C.; Griffin, J. M.; Yates, J. R.; Perez-Torralba, M.; Maria, M. D. S.; Webber, A. L.; Beaumont, M. L. L.; Samoson, A.; Claramunt, R. M.; Pickard, C. J.; Brown, S. P. *J. Am. Chem. Soc.* **2008**, *130*, 945.
(57) Bryce, D. L.; Bultz, E. B. *Chem.−Eur. J.* **2007**, *13*, 4786.
(58) Harris, R. K.; Joyce, S. A.; Pickard, C. J.; Cadars, S.; Emsley, L. *Phys. Chem. Chem. Phys.* **2006**, *8*, 137.
(59) Ashbrook, S. E.; Berry, A. J.; Frost, D. J.; Gregorovic, A.; Pickard, C. J.; Readman, J. E.; Wimperis, S. *J. Am. Chem. Soc.* **2007**, *129*, 13213.
(60) Pickard, C. J.; Salager, E.; Pintacuda, G.; Elena, B.; Emsley, L. *J. Am. Chem. Soc.* **2007**, *129*, 8932.
(61) Pourpoint, F.; Gervais, C.; Bonhomme-Coury, L.; Azaïs, T.; Coelho, C.; Mauri, F.; Alonso, B.; Babonneau, F.; Bonhomme, C. *Appl. Magn. Reson.* **2007**, *32*, 435.
(62) Joyce, S. A.; Yates, J. R.; Pickard, C. J.; Mauri, F. *J. Chem. Phys.* **2007**, *127*, 2041071.
(63) Joyce, S. A.; Yates, J. R.; Pickard, C. J.; Brown, S. P. *J. Am. Chem. Soc.* **2008**, *130*, 12663.

be suitable for the evaluation of ^{43}Ca NMR parameters of other Ca-organic materials, meaning that they should soon find broader applications for the elucidation of the local electronic environment around calcium sites in a wide range of materials, whether they are inorganic,[10] organic[14] or hybrid.

In this first part, we have shown that when calcium is surrounded by carboxylate and water ligands, and when the ^{43}Ca quadrupolar coupling constant is weak (C_Q < 1.5 MHz), as it is often the case in such environments (and thus most probably in biological sites),[23] both CSA and quadrupolar interactions can have a strong influence on the ^{43}Ca NMR static lineshapes, and must be considered to fully interpret the spectra. This is all the more important to bear in mind, because experiments carried out on samples with dilute calcium sites are likely to be performed at very high magnetic fields to increase sensitivity, meaning that lineshapes in which the CSA interaction becomes predominant might well be observed, as illustrated in the simulation of the ^{43}Ca static NMR spectrum of $Ca(C_6H_5COO)_2 \cdot 3H_2O$ at 21.1 T (Figure S5).

2. Analysis of the Coordination Environment of Calcium Using High Resolution ^{43}Ca−^{13}C NMR Spectroscopy. In contrast with inorganic calcium-containing samples such as hydroxyapatite,[30,32] in which information on the relative calcium-proton proximities is easy to access using ^{43}Ca−^{1}H correlation experiments (because of the simplicity of the ^{1}H NMR spectra), organic complexes like $*Ca(C_6H_5COO)_2 \cdot 3H_2O$ or calcium-proteins are expected to be much more difficult to study using such experiments, because of the lack of resolution in the ^{1}H NMR dimension. However, given that the ^{13}C MAS NMR spectra generally display more resolved resonances, high resolution ^{43}Ca−^{13}C NMR studies are expected to provide information more readily on the coordination environment around calcium in these samples.

The ^{13}C{^{1}H} CP MAS NMR spectrum of $*Ca(C_6H_5COO)_2 \cdot 3H_2O$ is shown in Figure 4. Two distinct resonances for the COO^- groups are observed at 174.4 and 172.8 ppm, in agreement with the presence of two distinct benzoates in the crystal structure. These were respectively assigned to C_7 and C_{17} by varying the CP contact time, because of the difference in ^{1}H environments of these carbons (Figure S6). The ^{13}C aromatic peaks are centered at 135.2, 130.0, and 126.5 ppm. In order to help assign these resonances, calculations of the ^{13}C chemical shifts were carried out using the GIPAW method (see Table 1). As shown in Figure 4, the calculated ^{13}C spectrum is in excellent agreement with the experimental one, with notably three distinct δ_{iso} ranges for the aromatic carbons and two resolved carboxylate resonances. These calculations show that the signal at 135.2 ppm corresponds to the C_{11} aromatic carbon, and confirm the relative isotropic shifts of C_7 and C_{17} (see Table 1 and Figure S6), as well as the purity of the sample prepared.

A wide range of Ca···C distances can be found in the structure, resulting in a large variety of Ca−C dipolar couplings (see Table S3). The closest carbon atoms are those belonging to the carboxylate groups directly bound to the calcium, which are labeled C_7. They are located at distances of 2.89, 3.52, and 3.60 Å, meaning that the corresponding ^{43}Ca−^{13}C dipolar couplings are 84, 47, and 44 Hz, respectively. In contrast, and as a characteristic example, the C_{11} carbons belonging to the uncoordinated benzoate are all located at distances >5.6 Å, and the ^{43}Ca−^{13}C dipolar couplings are thus <11 Hz! To the best of our knowledge, the possibility of probing experimentally such weak dipolar couplings between spin 1/2 and quadrupolar nuclei had not yet been investigated, and the purpose of this study was thus to try to analyze them.

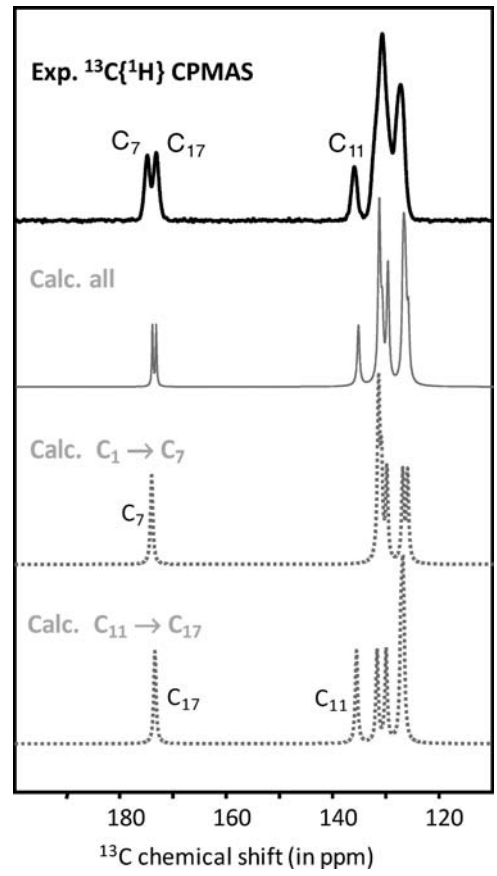

Figure 4. ^{13}C{^{1}H} CP MAS NMR spectrum of $*Ca(C_6H_5COO)_2 \cdot 3H_2O$. ^{13}C{^{1}H} CP MAS NMR spectrum of $*Ca(C_6H_5COO)_2 \cdot 3H_2O$ recorded at 11.75 T (top), and corresponding GIPAW calculated spectrum (bottom, with the contributions of the two distinct carboxylate anions). Only the isotropic resonances are shown. The numbering of the carbon atoms refers to Figure 1.

Table 1. ^{43}Ca and ^{13}C Isotropic and Anisotropic GIPAW Calculated NMR Parameters for $Ca(C_6H_5COO)_2 \cdot 3H_2O$[a]

	δ_{iso}	δ_{11}	δ_{22}	δ_{33}
Ca	6.3	16.6	11.2	−9.1
C_1	131.5	226.1	152.1	16.2
C_2	131.4	235.2	164.6	−5.6
C_3	126.0	234.8	145.7	−2.5
C_4	129.9	242.2	152.7	−5.1
C_5	126.9	237.4	146.9	−3.8
C_6	130.9	236.2	164.7	−8.3
C_7	174.2	229.6	185.0	108.0
C_{11}	135.4	231.5	160.2	14.6
C_{12}	129.8	235.2	160.7	−6.6
C_{13}	126.5	235.6	145.7	−1.7
C_{14}	127.0	237.4	146.2	−2.7
C_{15}	126.7	236.0	143.9	0.0
C_{16}	131.5	236.4	162.0	−3.9
C_{17}	173.5	238.0	179.7	103.0

[a] δ values are in ppm. δ_{11}, δ_{22}, δ_{33} are defined by $|\delta_{33} - \delta_{iso}| \geq |\delta_{11} - \delta_{iso}| \geq |\delta_{22} - \delta_{iso}|$, and $\delta_{iso} = 1/3(\delta_{11} + \delta_{22} + \delta_{33})$. For the ^{43}Ca site, the calculated quadrupolar parameters were C_Q = 0.87 MHz and η_Q = 0.81.

The first experimental evidence of the presence of residual ^{43}Ca···^{13}C dipolar couplings is obtained by comparing the static spectra of $*Ca(C_6H_5COO)_2 \cdot 3H_2O$ and the ^{13}C-labeled analogue $*Ca(C_6H_5*COO)_2 \cdot 3H_2O$ at 11.75 T: slight differences are noticeable on the high-frequency side of the signal (Figure 5c

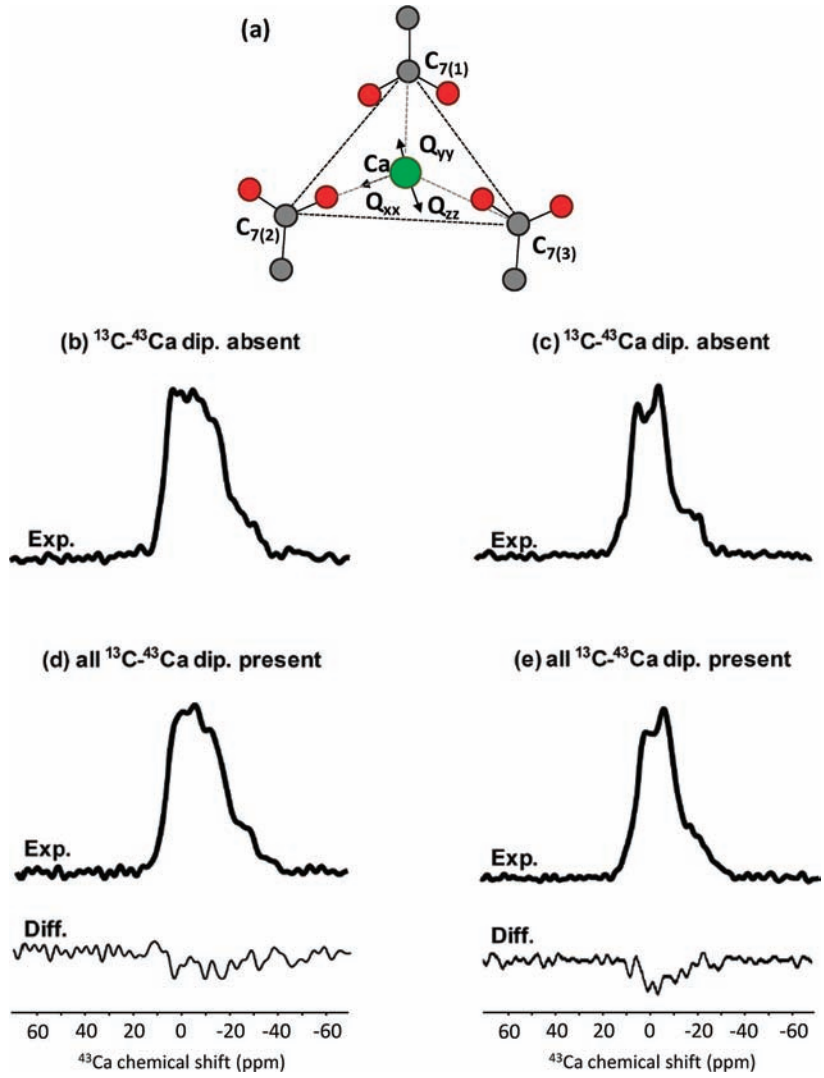

Figure 5. ^{43}Ca static NMR spectra of $*Ca(C_6H_5COO)_2 \cdot 3H_2O$ and $*Ca(C_6H_5*COO)_2 \cdot 3H_2O$. (a) Representation of the Ca site, with the nearest C atoms ($C_{7(i)}$) and the ^{43}Ca quadrupolar PAS. (b) ^{43}Ca static NMR spectrum of $*Ca(C_6H_5*COO)_2 \cdot 3H_2O$ at 9.4 T, recorded with ^{1}H and ^{13}C decoupling. (c) ^{43}Ca static NMR spectrum of $*Ca(C_6H_5COO)_2 \cdot 3H_2O$ at 11.75 T, recorded with ^{1}H decoupling. (d) and (e): ^{43}Ca static NMR spectra at of $*Ca(C_6H_5*COO)_2 \cdot 3H_2O$ at 9.4 and 11.75 T, respectively, recorded with ^{1}H decoupling only. The differences (b−d) and (c−e) are also shown below the spectra.

and 5e). A similar observation is made when comparing the static spectra of $*Ca(C_6H_5*COO)_2 \cdot 3H_2O$ recorded at 9.4 T, with and without ^{13}C decoupling (Figures 5b and 5d). Despite their weakness, residual $^{43}Ca-^{13}C$ dipolar couplings can slightly alter the static lineshapes. Several simulations were thus performed to try to analyze in more detail these weak interactions (Figures S7 and S8). Preliminary tests revealed that only the strongest residual dipolar coupling ($D(^{43}Ca-^{13}C_{7(1)}) = 84$ Hz) had an effect on the static ^{43}Ca NMR line shape, and the best fit was obtained for $\{\alpha_D,\beta_D\} \approx \{95°,95°\}$ at 9.4 T (Figure S8c), in rather good agreement with the dipolar angles calculated by GIPAW ($\{\alpha_D,\beta_D\} = \{107°, 132°\}$). Additional simulations were then carried out, revealing that changes in $\{\alpha_D,\beta_D\}$ or $D(^{43}Ca-^{13}C)$ can indeed very slightly alter the static line shape (Figures S8c to S8g), for instance when overestimating the intensity of the interaction ($D(^{43}Ca-^{13}C) = 150$ Hz, Figure S8g). Nevertheless, all in all, no precise estimation of the intensity of the $^{43}Ca-^{13}C$ dipolar coupling (and thus of the Ca···C distance) can be obtained from the static spectra, and no information on the position of the other nearby carbon atoms can be reached. Thus, in order to access the arrangement of organic ligands around Ca^{2+}, it appears necessary to implement other high resolution $^{43}Ca-^{13}C$ NMR experiments, which analyze differences in the local environment of ^{13}C spins.

2.1. Investigation of $^{43}Ca-^{13}C$ Proximities using $^{13}C-^{43}Ca$ TRAPDOR Experiments: Reaching Distances beyond 5 Å. First, experiments aimed at discriminating the different $^{13}C-^{43}Ca$ proximities in the sample were carried out. The TRAPDOR sequence was used, because it is known to be particularly robust for the investigation of dipolar couplings between spin-$^1/_2$ and quadrupolar nuclei.[21,39] Results of the $^{13}C\{^{43}Ca\}$ TRAPDOR study of $*Ca(C_6H_5COO)_2 \cdot 3H_2O$ are shown in Figure 6a. The strongest dephasing concerns the carboxylate resonance at 174.4 ppm, meaning that this signal corresponds to the carbon atom which is closest to the calcium, that is, C_7. This assignment is in complete agreement with the results of the GIPAW calculations. Interestingly, all the other ^{13}C resonances are also dephased in the presence of "long" ^{43}Ca recoupling pulses. This is all the more remarkable for the signal at 135.2 ppm (C_{11}), because the shortest $Ca-C_{11}$ distance is ~5.64 Å! Indeed, it shows that $^{43}Ca\cdots^{13}C$ dipolar couplings <11 Hz can be evidenced, which is *much weaker* than the $^{43}Ca-^{1}H$ dipolar couplings previously evidenced in hydroxyapatite.[30]

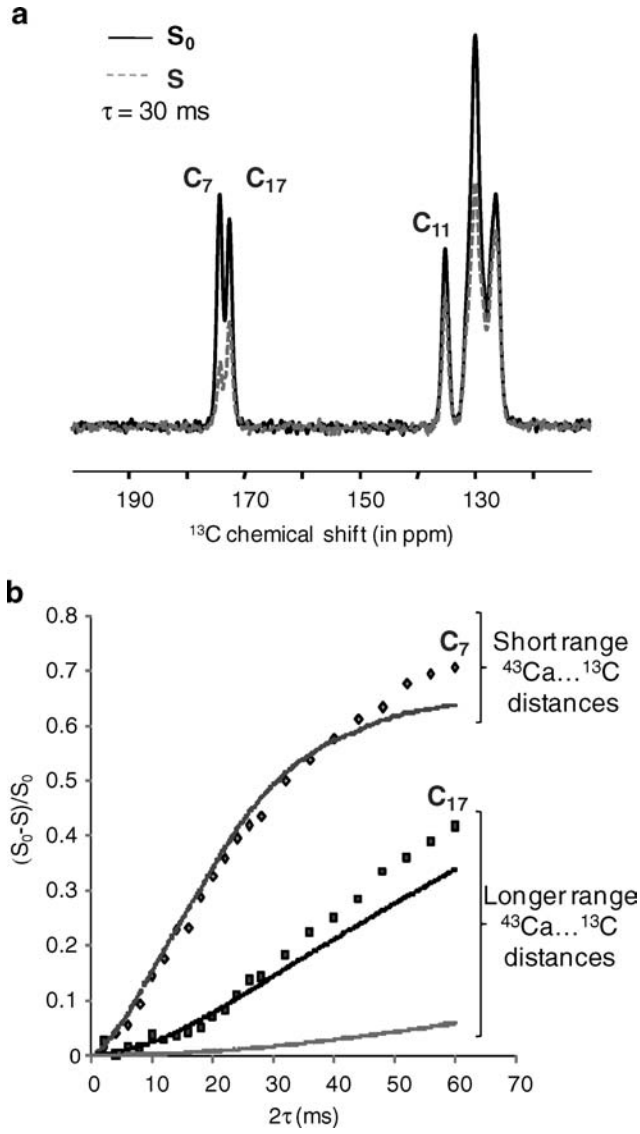

Figure 6. Results of $^{1}H-^{13}C-^{43}Ca$ TRAPDOR experiments performed at 9.4 T for $*Ca(C_6H_5COO)_2 \cdot 3H_2O$. (a) Comparison of the control (no ^{43}Ca irradiation, S_0) and double resonance (^{43}Ca irradiation, S) spectra for a recoupling time τ of 30 ms. (b) Experimental evolution of the normalized difference $(S_0 - S)/S_0$ as a function of the recoupling time τ for the carboxylate resonances C_7 and C_{17}, and simulation of the TRAPDOR buildup curves expected for short-range Ca···C correlations (dipolar couplings of 105 Hz, gray curve) and longer range Ca···C distances (dipolar couplings of 35 and 10 Hz in black and light gray, respectively).

The relative dephasing of the different ^{13}C resonances is also found to be in perfect agreement with the crystal structure and GIPAW assignments. Indeed, as shown on the TRAPDOR build-up curves in Figure 6b, the recoupling periods necessary to dephase the distant C_{17} carbon atoms are longer than for C_7. Similarly, a much smaller dephasing is observed for the aromatic signal centered at ~126.5 ppm which comes from carbon atoms all located at distances >5.24 Å (C_3, C_5, C_{13}, C_{14} and C_{15}), than for the signal at ~130.0 ppm, which notably comes from C_1, C_2 and C_6, which are much closer to calcium (see Table S3 and Figure S1). $^{13}C\{^{43}Ca\}$ TRAPDOR buildups were simulated, considering both short-range and long-range Ca−C interactions. The curves obtained for $^{43}Ca-^{13}C$ dipolar couplings of 10, 35, and 105 Hz are shown in Figure 6b. The latter two values were chosen for the simulations, because they respectively correspond to the root-sum-square of $^{43}Ca-^{13}C$ dipolar couplings for the individual C_{17} and C_7, which gives a "crude" approximation of the total $^{43}Ca-^{13}C$ dipole contribution. Very good agreement between the experimental and simulated dephasing curves was obtained for both carboxylate carbons, confirming that TRAPDOR experiments are perfectly suited for investigating both short- and long-range Ca···C distances, and can be used to estimate average $^{43}Ca-^{13}C$ dipolar couplings.

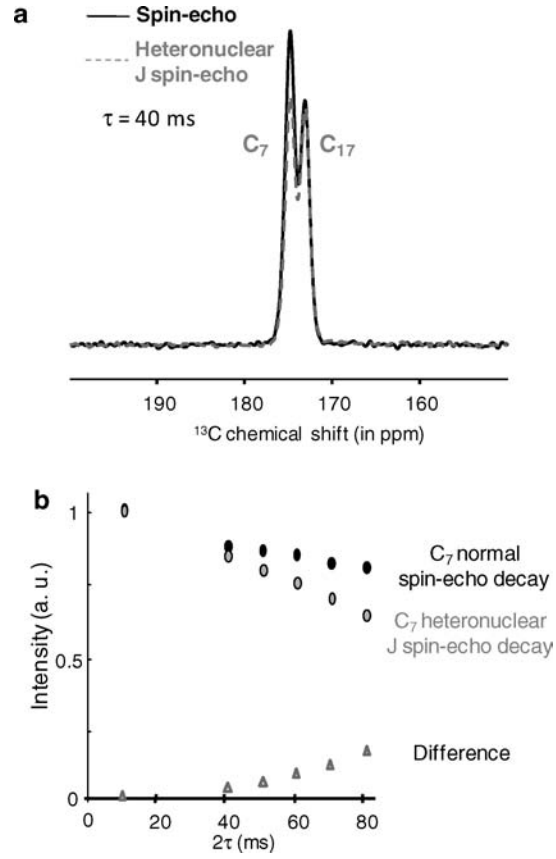

Figure 7. Results of $^{13}C-^{43}Ca$ heteronuclear spin−echo experiments performed at 9.4 T for $*Ca(C_6H_5*COO)_2 \cdot 3H_2O$. (a) Comparison of the normal spin−echo (no ^{43}Ca irradiation, solid line) and double resonance heteronuclear spin−echo (^{43}Ca irradiation, dashed gray line) spectra for a recoupling time τ of 40 ms. (b) Evolution in intensity of the C_7 resonance as a function of the evolution time τ.

2.2. Investigation of $^{43}Ca-^{13}C$ Through-Bond Connectivities using $^{13}C-^{43}Ca$ Heteronuclear *J*-Spin−Echoes. To examine the possibility of analyzing the local environment of calcium in more complex materials, additional NMR experiments were carried out to see whether through-bond connectivities between ^{13}C and ^{43}Ca (i.e., $^{43}Ca-O-^{13}C$ *J*-couplings) could also be observed. A $^{13}C/^{43}Ca$ heteronuclear *J*-spin−echo ($\tau-\pi-\tau$) experiment was first tested on the doubly labeled sample $*Ca(C_6H_5*COO)_2 \cdot 3H_2O$, in the prospect of distinguishing the ^{13}C resonances of C_7 and C_{17}, because they correspond to carboxylate groups coordinated and uncoordinated to the calcium, respectively. As shown in Figure 7, the intensity of the ^{13}C echo signal of C_7 decreases by application of a selective π pulse on the ^{43}Ca channel, whereas no effect is observed for C_{17}, even after echo delays (τ) as long as 40 ms. It is noteworthy that similar observations were made on the $*Ca(C_6H_5COO)_2 \cdot 3H_2O$ analogue for $\tau \approx 30$ ms. These observations could reflect the presence of a *J*-coupling interaction between ^{43}Ca and C_7 (and thus a Ca−O−C_7 connectivity). Indeed, the other possible contributions to the dephasing of the C_7 peak, such as remaining $^{43}Ca-^{13}C$ dipolar couplings or residual quadrupole-dipole

interaction terms, should be negligible under these conditions (see Supporting Information, section C2). However, no attempt to precisely measure this supposed *J*-coupling term was made here. Indeed, due to the weakness of the C_7 dephasing (Figure 7b), much longer τ delays would have been necessary to measure this interaction, meaning that much longer ^1H decoupling periods would have been used, thus significantly increasing the possibility of damaging the probe. Nevertheless, although additional experiments (using for example probes using the Hall-effect to set the magic angle[64]—to further ensure the total suppression of the residual interactions mentioned above—and/or fast MAS probes, to ensure a more complete suppression of any residual homonuclear interactions), as well as DFT calculations[62,63] would need to be carried out to unambiguously prove the presence of a $^{13}C-^{43}Ca$ heteronuclear *J*-coupling, the results here show that very simple NMR experiments like heteronuclear *J*-spin−echoes allow differences in $^{13}C-^{43}Ca$ interactions to be revealed.

In this second part, we have shown that $^{13}C-^{43}Ca$ interactions can readily be studied by different double resonance solid state NMR experiments, and that the presence of carbon atoms located at ∼5.5 Å can be evidenced using very simple experiments like TRAPDOR. This underscores that a detailed picture of the coordination environment of calcium can potentially be reached, by evaluating the different Ca···C distances, and their more quantitative estimation could also well be carried out using the REAPDOR sequence (rotational-echo adiabatic-passage double-resonance).[65] Therefore, $^1H-^{13}C-^{43}Ca$ experiments certainly appear to be a valuable tool for investigation for Ca-containing biomolecules and biomaterials.

Conclusion

The high resolution ^{43}Ca solid state NMR studies presented here open new perspectives for the analysis of calcium sites in biological materials. Indeed, in addition to ^{43}Ca isotropic chemical shifts and quadrupole coupling constants, which had already been shown to provide some information on the local structure around calcium,[23] it was demonstrated here that further details on the electronic environment of ^{43}Ca can be obtained by recording ^{43}Ca static solid state NMR spectra, because the spectral features are very sensitive to the magnitude and orientation of the ^{43}Ca CSA and quadrupolar tensors. It was also shown that information on the relative position of the different molecules and anions which are in the vicinity of Ca^{2+} can be obtained through high resolution $^{43}Ca-^{13}C$ double resonance experiments, such as TRAPDOR and heteronuclear *J*-spin−echoes. In particular, at this stage, $^{43}Ca-^{13}C$ TRAPDOR appears as a *unique* alternative to other techniques like XRD or EXAFS, as it can readily provide qualitative information on the different Ca···C distances in a sample, well beyond the first coordination sphere of calcium, and has the advantage of being very robust and easy to implement.

Although the NMR studies were performed here on ∼100 mg of 60% ^{43}Ca-labeled $*Ca(C_6H_5COO)_2 \cdot 3H_2O$, it is noteworthy that all experiments were carried out with "standard" NMR equipment (4 mm rotor MAS triple-resonance probe, 9.4 T magnet), and that in these conditions, only ∼9 h were necessary to record each TRAPDOR spectrum. Thus, by working at higher magnetic fields, it should become possible to carry out similar experiments on a wide range of compounds, in particular those containing lower concentrations of ^{43}Ca, due to the higher dilution of calcium sites, or the lower (and thus less expensive) enrichment level used in the syntheses. In particular, it can be predicted that using smaller-volume rotors, but much higher magnetic fields (e.g., 21 T), qualitative information on Ca···C distances in 60% ^{43}Ca-labeled samples of small metalloproteins like calmodulin will become accessible, and should help rationalize a wide range of biological processes involving calcium. This is all the more important since so far, structural studies of poorly crystalline proteins have mainly focused on understanding the structure of the amino acid backbone (using for instance high resolution $^1H/^{15}N/^{13}C$ solid state NMR experiments),[66,67] without any *direct* information on the Ca^{2+} binding sites. Furthermore, because $^{43}Ca-^{13}C$ spin pairs are present in a very wide range of materials, this work should also help understand the importance of carbonate substituents in the mineral phase of bone,[68] the hydration behavior of pharmaceutical materials like fenopren calcium,[69] and even natural phenomena like biomineralisation, in which one of the key steps is the interaction of Ca^{2+} with organic templates.[70]

As demonstrated above, using long TRAPDOR recoupling periods, correlations between calcium and carbon atoms separated by more than 5.6 Å can be evidenced. This proves that long-range distances between spin-$^1/_2$ and quadrupolar nuclei are detectable. As a result, similar studies should also allow $^{43}Ca\cdots^{31}P$, $^{43}Ca\cdots^{29}Si$ or even $^{43}Ca\cdots^{15}N$ proximities to be detected, provided that efficient ^1H heteronuclear decoupling and sufficiently fast MAS conditions are used, in order to remove any residual dipolar coupling and allow long enough T_2' values to be reached for the spin-$^1/_2$ nucleus. The possibility of analyzing different ranges of Ca−P and Ca−Si distances should be of great benefit for materials science, as it could help understand the structure of a wide range of compounds, by identifying which phosphates or silicates are directly bound to Ca^{2+}. Additionally, information on calcium−nitrogen proximities could help gain further knowledge on the structure of calcium sites in proteins. Finally, because of the robustness of TRAPDOR sequence, it can be expected that similar studies should also be transferable to other low-γ quadrupolar nuclei commonly found in metalloproteins, such as ^{25}Mg or ^{67}Zn, thus opening new perspectives on the understanding of their biological role.

Acknowledgment. EPSRC, AWM and the University of Warwick are acknowledged for partial funding of the NMR work at Warwick. D.L. thanks the 6th European Community Framework Program for a Marie Curie Intra-European Fellowship, and AW NSERC for a Canadian PDF. Calculations were performed on the IDRIS supercomputer centre of the CNRS (Project 81461).

Supporting Information Available: *Section A.* Figure S1. Details of the crystal structure of $[Ca(C_6H_5COO)_2]\cdot 3H_2O$. Figure S2. IR and XRD characterization of $[*Ca(C_6H_5*COO)_2]\cdot 3H_2O$. Figure S3. Experimental and simulated ^{43}Ca MAS NMR spectra of $*CaCO_3$, for the setting of the magic angle. Figure S4. Details of the $^{13}C-^{43}Ca$ MAS NMR pulse sequences. Figure S5.

(64) Mamone, S.; Dorsch, A.; Johannessen, O. G.; Naik, M. V.; Madhu, P. K.; Levitt, M. H. *J. Magn. Reson.* **2008**, *190*, 135.
(65) Gullion, T. *Chem. Phys. Lett.* **1995**, *246*, 325.
(66) Böckmann, A. *Magn. Reson. Chem.* **2007**, *45*, S24, and references therein.
(67) Chen, L.; Kaiser, J. M.; Lai, J.; Polenova, T.; Yang, J.; Rienstra, C. M.; Müller, L. J. *Magn. Reson. Chem.* **2007**, *45*, S584.
(68) Elliott, J. C. *Structure and Chemistry of the apatites and other calcium phosphates*; Elsevier: Amsterdam, 1994.
(69) Zhu, H.; Xu, J.; Varlashkin, P.; Long, S.; Kidd, C. *J. Pharmaceut. Sci.* **2001**, *90*, 845.
(70) Arias, J. L.; Fernandez, M. S. *Chem. Rev.* **2008**, *108*, 4475.

Simulations of static ^{43}Ca NMR spectra at 21.1 T. Figure S6. Assignment of the carboxylate resonances of [*Ca($C_6H_5COO)_2$]·$3H_2O$ by $^{13}C\{^1H\}$ CP MAS NMR, by variation of the contact time. Figure S7. Int2Q_D simulations of static ^{43}Ca NMR spectra at 9.4 T, with and without one $^{13}C-^{43}Ca$ dipolar coupling. Figure S8. Experimental static ^{43}Ca NMR spectra of [*Ca(C_6H_5*$COO)_2$]·$3H_2O$ at 9.4 T with or without ^{13}C decoupling, and Int2Q_D simulations including the strongest $^{13}C-^{43}Ca$ dipolar coupling, with different $\{\alpha_D,\beta_D\}$ Euler angles and different D($^{13}C-^{43}Ca$) values. ***Section B.*** Table S1. Summary of the experimental conditions used to record the ^{43}Ca static and MAS NMR spectra. Table S2. Fractional atomic coordinates of Ca($C_6H_5COO)_2$·$3H_2O$ after relaxation of the proton positions using DFT calculations. Table S3. Ca···C distances in the crystal structure of [Ca($C_6H_5COO)_2$]·$3H_2O$ and corresponding dipolar couplings. ***Section C.*** C1. Experimental details related to the simulations and the SIMPSON, dmfit and Int2Q_D softwares. C2. Discussion on the heteronuclear *J*-spin−echo experiments. This material is available free of charge via the Internet at http://pubs.acs.org.

JA904553Q